

TWO-DIMENSIONAL ANGULAR SIZE OF A SYNCHROTRON LIGHT PATTERN
AS A FUNCTION OF WAVELENGTH *

Daryl Reagan
Stanford Linear Accelerator Center
Stanford University, Stanford, California 94305

ABSTRACT

Procedures are given for estimating the two dimensions of the angular size of a synchrotron light pattern as a function of wavelength for each of two polarization components. It is found that horizontal angular sizes (measured in the orbital plane) are substantially larger than corresponding vertical angular sizes. Except for wavelengths which are considerably smaller than a critical wavelength, a relativistic electron with bending radius R emits radiation with wavelength λ into a pattern which has angular dimensions of order $(\lambda/R)^{1/3}$.

Submitted to Review of Scientific Instruments

* Work supported by the Department of Energy, contract DE-AC03-76SF00515.

INTRODUCTION

To predict the resolving power of an electron beam momentum spectrum monitor¹ which uses synchrotron light, it was desired to estimate the horizontal width of the angular distribution of the visible light observed when an electron moves in a horizontal plane through a uniform vertical magnetic field. A knowledge of the horizontal spread may also be of value to users of synchrotron light and x-rays from storage rings. This interest reflects changes in experimental apparatus since 1949 when Schwinger² remarked that the distribution in the horizontal angle was unobservable in practice.

Direct observation remains difficult, but there is an experimentally observed effect of horizontal divergence that is beneficial. Suppose the horizontal angular width were as small as $1/\gamma$, the ratio of rest energy to total energy of the radiating electron, for any wavelength, λ . If so, a profile monitor situated a distance L from a source could have effective horizontal aperture at most $\sim L/\gamma$, angular resolution no better than $\sim \lambda\gamma/L$, and space resolution no better than $\sim \lambda\gamma$. At PEP, profile monitors have $\lambda\gamma \approx 1.8$ cm, but resolution is probably finer than the minimum observed horizontal spot size, which is $2\sigma \approx 4$ mm (Ref. 3).

To clarify the idea of horizontal angular width, imagine that a sinusoidally oscillating dipole D is moving at a constant speed near that of light in a circular path with radius R in a horizontal plane which includes a distant observer O , as in Fig. 1. Let the wavelength of the signal received at O have some minimum value $\lambda_m \ll R$ for the parts of the wavetrain which originated near T . Transit time differences will cause other parts of the wavetrain to differ in phase by $\phi \approx 2\pi R(\chi - \sin\chi)/\lambda_m \approx \pi R\chi^3/3\lambda_m$ from

those originating near T. When $\chi > (3\lambda_m/R)^{1/3}$, the relative phase shift will exceed π and will grow more and more rapidly with further increases in χ . Radiation emitted at angles $|\chi| \gg (3\lambda_m/R)^{1/3}$ and detected at 0 will thus have a quality which is akin to incoherence.

A FORMULA DUE TO SCHWINGER

Schwinger's paper² gives expressions from which the two-dimensional angular distribution of synchrotron light may be estimated for a specified wavelength. His Eq. (II.31) is

$$P(\psi, \omega, t) = \frac{-e^2 \omega^2}{4\pi^2 R \omega_0^2} (1 - \beta^2 + \psi^2) \int_{-\infty}^{\infty} \left[1 - \beta^2 + \frac{1 - \beta^2 + \psi^2}{2} (x^2 + y^2 + 2xy) \right] \cdot \cos \left[\frac{\omega R}{2c} (1 - \beta^2 + \psi^2)^{3/2} \left(x + \frac{x^3}{3} + y + \frac{y^3}{3} \right) \right] dx dy \quad (1)$$

where ω is the angular frequency of the observed light, R is the radius of the electron orbit, $\omega_0 = c/R$, $\beta = v/c$, ψ is vertical angle, $x = (1 - \beta^2 + \psi^2)^{-1/2} \chi$, χ is horizontal angle, $y = (1 - \beta^2 + \psi^2)^{-1/2} c\tau/R$, and τ is the transit time of a light signal. If the indicated integration over y is done (Schwinger's Eqs. (II.10), (II.12), and (II.33) are helpful), and dx is replaced by $d\chi/(1 - \beta^2 + \psi^2)^{1/2}$, the results may be written as follows:

$$dP = \frac{e^2}{\lambda} \left(\frac{2^{2/3}}{3^{1/6} \pi^{1/3}} \frac{\psi^2}{\Omega^2} P_1 + \frac{\sqrt{3}}{\pi} P_2 \right) d\psi d\chi d\omega dt \quad (2a)$$

$$P_1 = \langle \cos\theta \rangle \xi^{1/3} K_{1/3}(\xi) \quad (2b)$$

$$P_2 = \langle x \sin\theta \rangle \xi K_{2/3}(\xi) \quad (2c)$$

$$\Omega = (\lambda/R)^{1/3} \quad (2d)$$

$$\xi = (\lambda_c/2\lambda) (1 + \gamma^2 \psi^2)^{3/2} \quad (2e)$$

$$\theta = 3\xi(x + x^3/3)/2 \quad (2f)$$

where λ is the wave length of the light, $\lambda_c = 4\pi R/3\gamma^3$, a critical wavelength, and the K's are Bessel functions.^{2,4} These expressions represent an intermediate step in reaching Schwinger's Eq. (II.32). They indicate that the angular distribution is symmetric with respect to the χ and ψ axes.

Since P_1 and P_2 represent power radiated away from an electron, and all the other terms in Eqs. (2b) and (2c) are positive, the averages $\langle \cos\theta \rangle$ and $\langle x \sin\theta \rangle$ must also be positive. This constrains the intervals in χ (or equivalently x or θ) over which physically meaningful averages may be computed. If intervals are marked off by $\theta = 0, 2n\pi, 4n\pi, 6n\pi$, etc., then it is possible to choose integral values of n for any given ξ that satisfy the condition that all values of $\langle \cos\theta \rangle$ and $\langle x \sin\theta \rangle$ must be positive.

Any average evaluated over such an interval is the algebraic sum of $2n$ positive and $2n$ negative numbers, each proportional to an integral over a quarter period of a distorted cosine or sine function. Except when both χ and ξ are small ($\theta \leq 2\pi$ and $\xi < 1$), the averages represent small differences. Grossly different shapes of computed P_1 and P_2 functions can result from other choices of end-points.

Indeed, the details of angular distributions will be influenced by interference effects due to the geometry of measuring apparatus as well as those due to the peculiarities of the radiation process.

The plots of P_1 and P_2 vs χ/Ω which follow are based upon computation in which $n=1$, so that the averages $\langle \cos\theta \rangle$ and $\langle x \sin\theta \rangle$ which are indicated all represent intervals in χ for which $\Delta\theta = 2\pi$. The extent to which the indicated widths of the angular distributions are sensitive to a choice of n may be judged upon inspection of the figures.

NUMERICAL RESULTS FOR P_1

Figure 2 gives values of P_2 which result from numerical integrations. P_1 represents vertically polarized light. If ξ_0 is not too large, the approximate range of ψ values (vertical angles) which include most of the vertically polarized light can be found from Fig. 3. To make an estimate, first evaluate $\xi_0 = \lambda_c/2\lambda = 2\pi R/3\lambda\gamma^3$. Then find $A_1(\xi_0)$ from Fig. 3, which will also indicate the value ξ_1 for which A_1 is (say) a factor of ten smaller. Now find the corresponding ψ_1 from Eq. (2e), which can be rewritten

$$\psi_1 = \left(\frac{3\xi_1}{2\pi} \right)^{1/3} \left[1 - \left(\frac{\xi_0}{\xi_1} \right)^{2/3} \right]^{1/2} \Omega \quad (3)$$

If $\xi_1 < 2$, then, according to Fig. 2, most of the light belonging to P_1 will be confined within the horizontal angular range $|\chi| < 1.5\Omega$. Equation (3) and Fig. 3 indicate that in many cases the range of ψ values which contribute important amounts of light to P_1 can be approximated by $|\psi| < (3\xi_1/2\pi)^{1/3}\Omega$. For cases where $\xi_1 < 2$, the χ -width of

P_1 is 1.5 to 2 times larger than the ψ -width. It can be shown that for sufficiently large χ , P_1 becomes proportional to the sixth power of $(1/\chi)$. Two-dimensional angular profiles of a vertically polarized light pattern are shown in Fig. 4a. The quantity Q_1 plotted in Fig. 4a is $Q_1 = 2^{2/3} \psi^2 P_1 / 3^{1/6} \pi^{1/3} \Omega^2$.

A MODEL FUNCTION FOR P_2

The function P_2 , given in Eq. (2c), describes the horizontally polarized part of the synchrotron light, which constitutes most of the light, is spread out more in χ , and decreases less rapidly with χ than does P_1 . An approximation can be found that represents P_2 well enough for some practical purposes. This is done by using power series approximations and a reversion formula to transform $x \sin \theta dx$ into a function of θ only and integrating the θ function over an interval of 2π in θ . To find the average, $\langle x \sin \theta \rangle$, it is necessary to divide the integral by a corresponding interval in x which is calculated by a similar procedure. The result is valid only for large x_1 :

$$\langle x \sin \theta \rangle \cong \frac{2}{3\xi x_1^2} \left[1 - \frac{3}{x_1^2} - \frac{8(21 - \pi^2)}{27\xi^2 x_1^6} \right],$$

where x_1 corresponds to the midpoint of the integration interval in θ .

The approximation for P_2 is then found by constructing a model function of x_1 that is a constant, $2/3 \xi x_0^2$, when x_1 is less than some value, x_0 , and is $2/3 \xi x_1^2$ for x_1 larger than x_0 . The value for x_0 can

be found by using the relation [Ref. 2, Eq. (II.12)]

$$\int_0^{\infty} x \sin \frac{3\xi}{2} \left(x + \frac{x^3}{3} \right) dx = \frac{1}{\sqrt{3}} K_{2/3}(\xi)$$

which must equal the corresponding integral of the model function. When x_1 is replaced by $\chi / (1 - \beta^2 + \psi^2)^{1/2}$, the results give the model function:

$$P_{2m} \cong \frac{1}{8} \xi^2 K_{2/3}^3(\xi) \quad , \quad \text{when } \chi < \chi_0 \quad , \quad (4a)$$

$$P_{2m} \cong \frac{1}{8} \xi^2 K_{2/3}^3(\xi) \frac{\chi_0^2}{\chi^2} \quad , \quad \text{when } \chi > \chi_0 \quad , \quad (4b)$$

with

$$\chi_0 = \left(\frac{3\lambda}{2\pi R} \right)^{1/3} \left[\frac{4}{\sqrt{3} \xi^{2/3} K_{2/3}(\xi)} \right] \approx \frac{1.805\Omega}{\xi^{2/3} K_{2/3}(\xi)} \quad . \quad (4c)$$

According to the model function, the limits $\pm\chi_0$ encompass half the light belonging to P_2 for each value of ψ . Figure 5 gives χ_0 in units of Ω as a function of ξ . Figure 3 gives values of $(\xi^2/8)K_{2/3}^3(\xi)$ vs ξ . Interesting values of ξ and ψ for P_2 can be found from Fig. 3 by a procedure which is similar to that outlined above for P_1 . Figure 6 gives comparisons between the model and the results of numerical computations of P_2 . The model is usually pretty good when $|\chi| > \chi_0$ and suffers its worst discrepancies in the neighborhood of $\xi = .5$, when it is about 20% high for $|\chi| = \chi_0$. The model is, of course, unsuitable for describing fine structure in P_2 for $|\chi| < \chi_0$. In the numerical calculations, the average, $\langle x \sin\theta \rangle$, was evaluated over intervals in χ in which θ advances from zero to 2π , 4π , 6π , etc.

Figure 4b shows some profiles of $Q_2 = \sqrt{3} P_2/\pi$ for visible light from a relativistic electron deflected with a 75 m bending radius.

DISCUSSION

This exercise has been prompted by an interest in a gross feature, namely the horizontal (χ) spread, of visible synchrotron light produced in a bending magnet (B13) in the beam switchyard at SLAC.⁵ In this case, most of the visible light belongs to $\xi < 1$. The results indicate that the light occupies a solid angle which is much wider, horizontally, than $1/\gamma$, but not much wider than 10 milliradians. A practical consequence is that some of the light can be focused into a good image which will be only slightly degraded by light originating upstream or downstream from the optical source plane.¹

Let it be emphasized, however, as suggested above, that when applied to synchrotron light, the term "angular distribution" can become adequately defined only when it is linked to a knowledge of the geometry of the apparatus by which the radiation is detected.

ACKNOWLEDGMENTS

I wish to acknowledge help and support given by the late K. B. Mallory, and to thank K. F. Crook for helpful criticism.

REFERENCES

1. D. Reagan and T. Hostetler, IRE Transactions on Nuclear Science, Vol. NS-26, No. 3, June 1979, p. 3297, and SLAC-PUB-2271.
2. J. Schwinger, Phys. Rev. 75, 1912 (1949).
3. A. Sabersky, SLAC-PUB-2683 (1981), and private communication.
4. G. N. Watson, Bessel Functions, MacMillan, New York, 1945;
Vaclav O. Kostroun, Nucl. Instrum. Methods 172, 371 (1980);
G. K. Green, BNL-50595, Vol. II, 1-72 (1977).
5. R. B. Neal, ed., The Stanford Two-Mile Accelerator,
W. A. Benjamin, Inc., New York, 1968, p. 586.

FIGURE CAPTIONS

Fig. 1. The difference between the two paths connecting T and O is $R(\chi - \sin\chi) \approx R\chi^3/6$.

Fig. 2. P_1 vs χ/Ω . P_1 has been numerically computed according to Eq. (2b), and represents the vertically polarized light. The angles are given in units of magnitude $\Omega = (\lambda/R)^{1/3}$. Percentages refer to fractions of total area.

Fig. 3. Central amplitudes of P_1 and P_{2m} as functions of ξ . A_1 is the average height of the part of the P_1 vs ξ plot (see Fig. 2) that contains 90% of the vertically polarized light. $A_2 = (\xi^2/8) K_{2/3}^3(\xi)$, and belongs to the horizontally polarized light (see Eqs. 4).

Fig. 4. Half-profiles for light of wavelength $0.6 \mu\text{m}$ from 10.2 GeV electrons with 75 m bending radius. Q_1 represents vertically polarized light and is found from numerical integrations. Q_2 represents horizontally polarized light and is estimated using Eqs. (4). Values of ξ are 3.27×10^{-5} , .0332, .263, .885 and 2.10 for $\psi = 0, 0.5, 1, 1.5$ and 2 mrad, respectively; $\Omega = 2\text{mrad}$.

Fig. 5. Horizontal half-width of the angular distribution of the horizontally polarized light as a function of ξ . See Eqs. (2e) and (4c).

Fig. 6. P_2 vs χ/Ω . P_2 is defined in Eq. (2c) and represents horizontally polarized light. Angles are scaled in units of $\Omega = (\lambda/R)^{1/3}$.

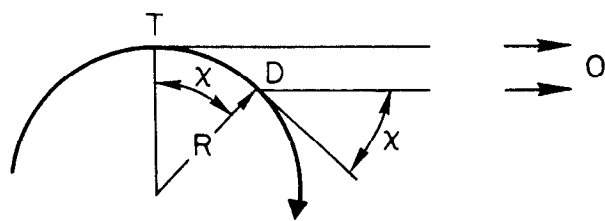


Fig. 1

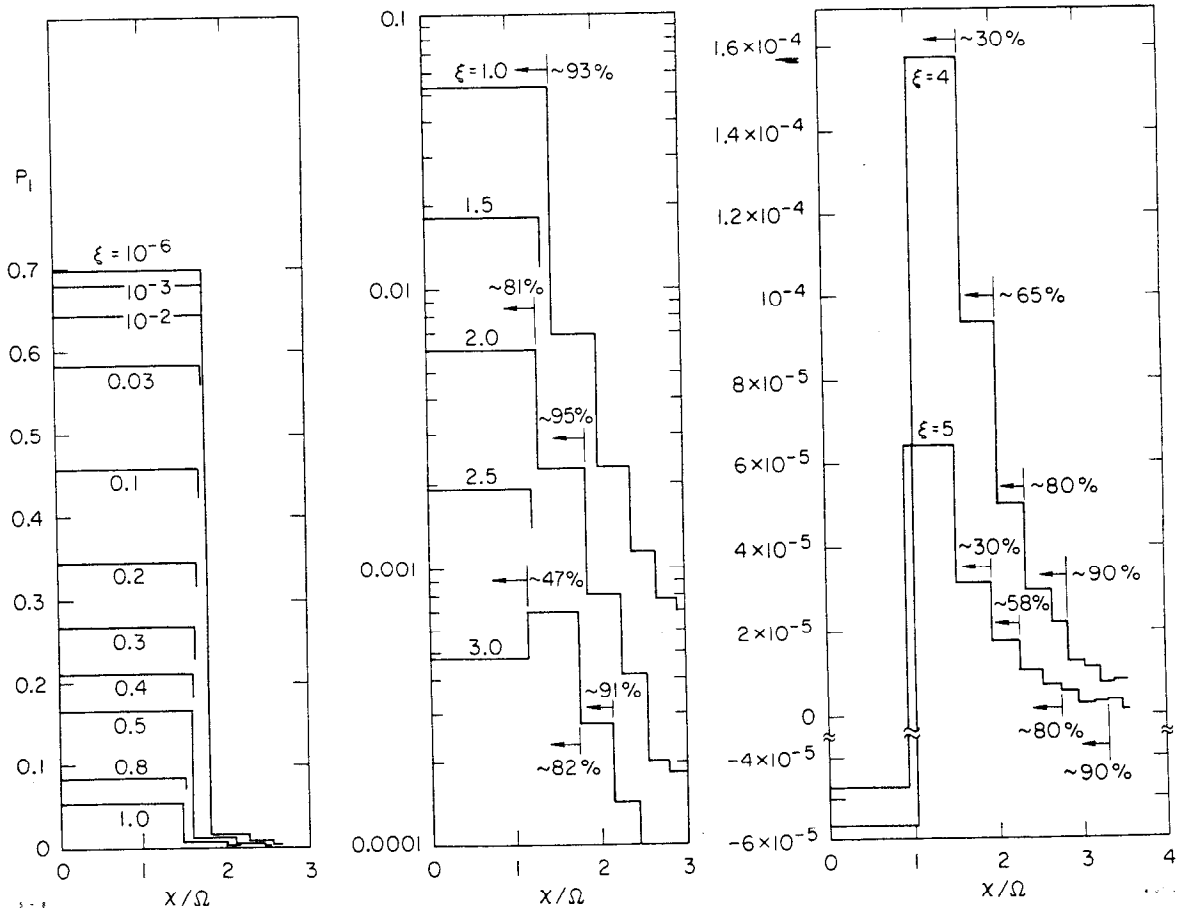


Fig. 2

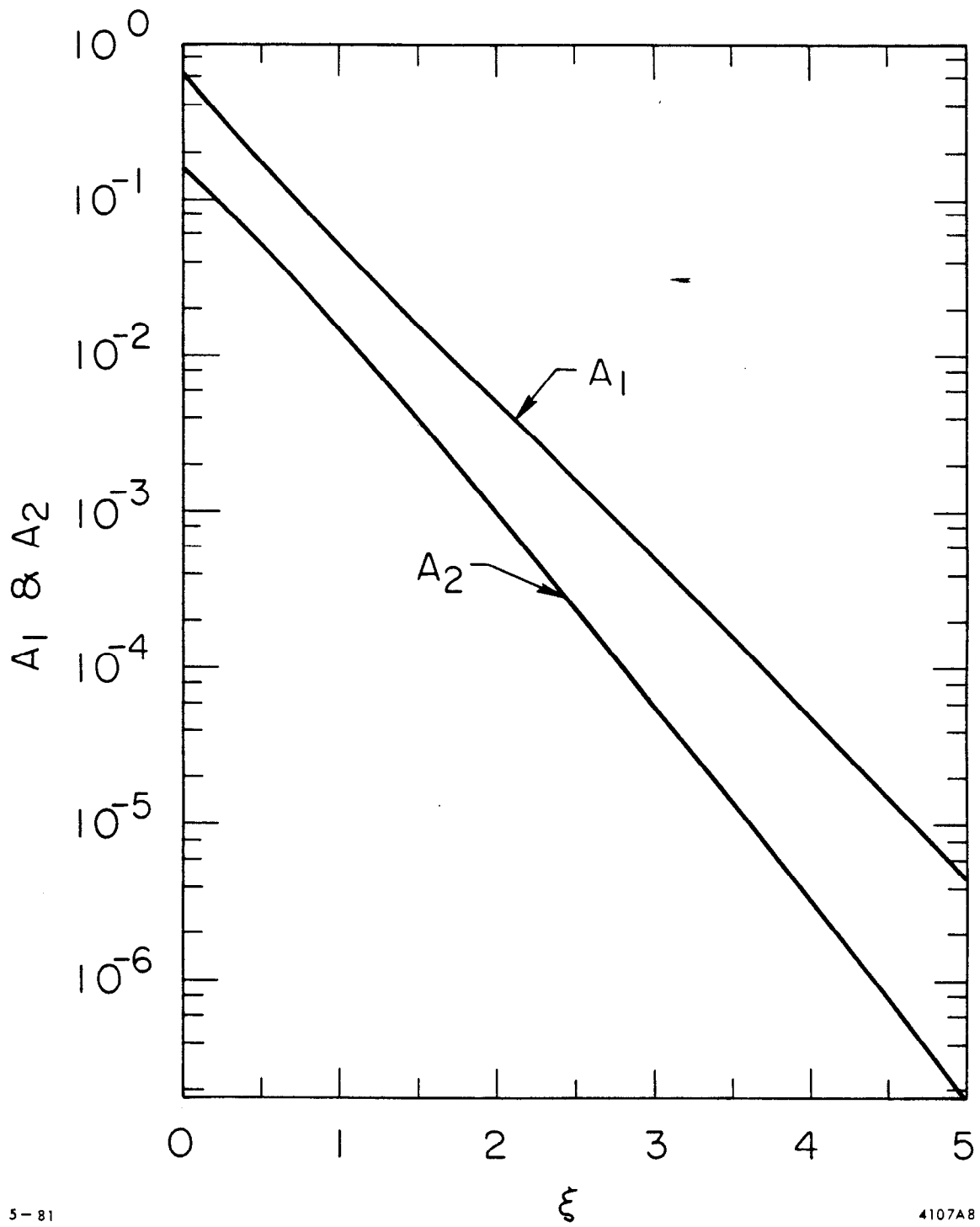


Fig. 3

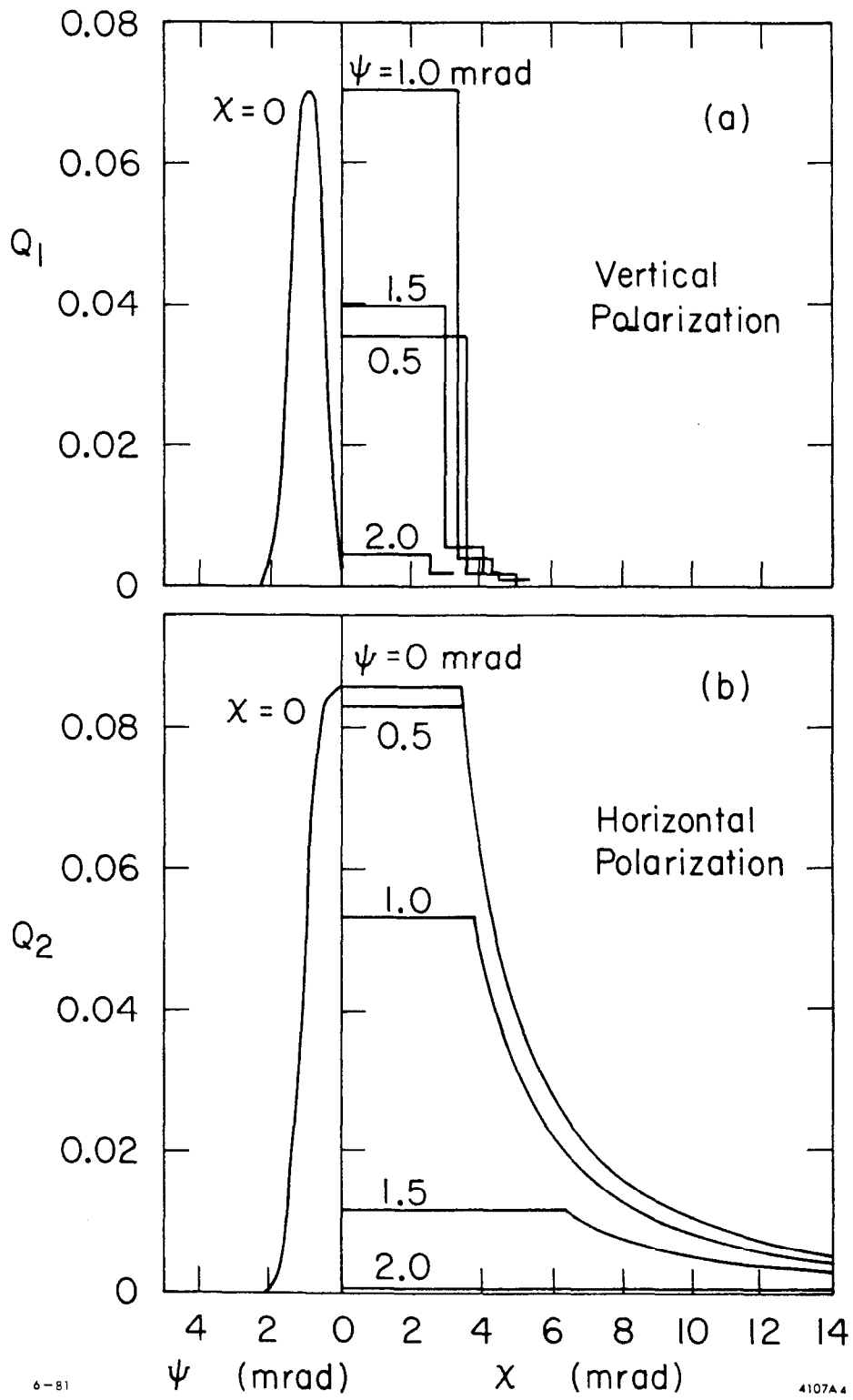


Fig. 4

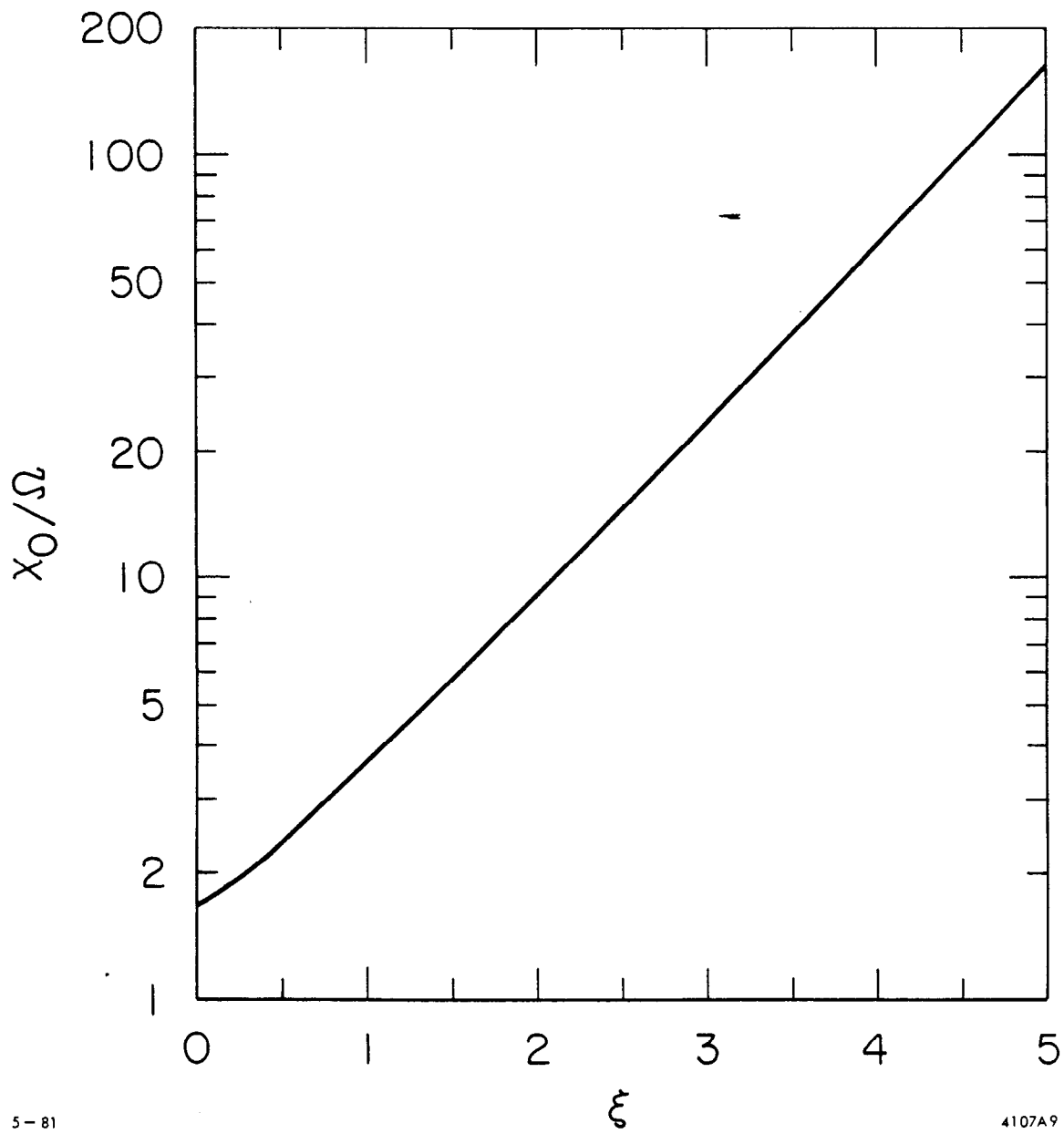


Fig. 5

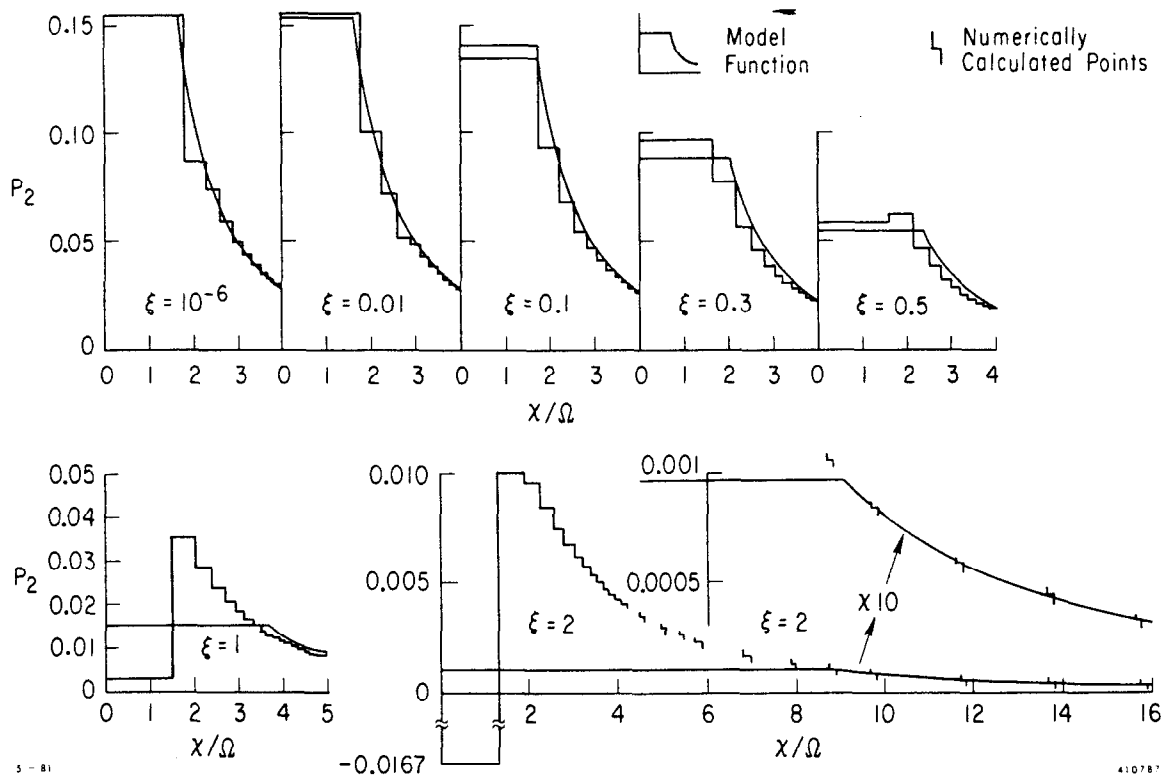


Fig. 6